Sub-bandgap luminescence centers in silicon created by self-ion implantation and thermal annealing

Yu Yang,[1,a)] Jiming Bao,[2] Chong Wang,[3,b)] and Michael J. Aziz[4]
[1]*Institute of optoelectronic information materials, Yunnan University, 2 Northern Cuihu Road, Kunming, Yunnan Province 650091, China*
[2]*Department of Electrical and Computer Engineering, University of Houston, 4800 Calhoun Road, Houston, Texas 77204, USA*
[3]*Institute of Engineering and Technology, Yunnan University, 2 Northern Cuihu Road, Kunming, Yunnan Province 650091, China*
[4]*School of Engineering and Applied Sciences, Harvard University, 29 Oxford Street, Cambridge, Massachusetts 02138, USA*

(Received 2 December 2009; accepted 27 April 2010; published online 18 June 2010)

We investigated the conditions for the generation of silicon sub-bandgap luminescence centers (W, R, and D1 centers) in p-type silicon wafer by self-ion implantation and thermal annealing. Luminescence centers and their spatial distributions were probed by measuring their photoluminescence (PL) spectra before and after sequential removal of top surface layers. It was demonstrated that the optimal annealing temperature for W-line is ~300 °C. The strongest R-line is observed in the sample with a dose of 10^{14} cm^{-2} and at an annealing temperature of 700 °C. The creation of D1-band requires a minimum dose of 3×10^{14} cm^{-2} and a minimum annealing temperature of 800 °C. PL versus etch depth measurements indicate that within the studied dose range, the W-line luminescence centers are distributed beyond twice the ion projected range (R_p ≈400 nm), R-line centers are located slightly deeper than the R_p, and D1 related defects are distributed at about the same depth as R_p. These results provide valuable information for fabricating the silicon-based infrared light sources. © *2010 American Institute of Physics*.
[doi:10.1063/1.3436572]

I. INTRODUCTION

Silicon-based infrared light-emitting diodes (LEDs) and lasers are the essential components for the realization of integrated optical-electronic circuits, i.e., silicon photonics, which holds the promise for the future in terms of fast computer chips and telecommunication applications.[1–4] However, because silicon is an indirect band-gap semiconductor, it is not a suitable material for efficient light emitters. Sub-bandgap near-infrared light emitters are desirable for silicon photonics due to their low optical propagation loss. Over the past decades, several techniques have been developed to transform silicon into an optically active material, including implantation of rare earth ions such as Er into Si,[1,5] introduction of external impurities that can form optically active defects,[6–10] and utilization of intrinsic defects in silicon.[8,11–15] Intrinsic point defects, defect clusters, and extended defects (such as dislocations) in silicon offer a rich emission spectrum for the applications as various infrared light sources.[16,17] The demonstration of D1-band and W-line LEDs,[12,14,18] especially the D1-line room temperature LED,[12,18] has shown the potential of utilizing intrinsic defects for highly-efficient room temperature silicon LEDs.

The implementation of integrated optic-electronic circuits requires the fabrication of silicon-based light emitters to be compatible with current silicon technology. Plastic deformation and direct silicon bonding (DSB) have been used to fabricate D1 LEDs.[12,15,18] These two techniques, especially plastic deformation, are not compatible with current silicon technology. In the DSB fabricated LEDs, dislocations are created at the bonding interface between silicon dioxide and silicon and serve as an active region of the LED.[15] In this case, the position and thickness of the dislocation-contained region cannot be well controlled, and carriers have to be tunneled through oxide barrier, which could result in degradation of device performance and low quantum efficiency. Ion implantation, which is a standard technique in silicon electronic manufacture, has therefore the practical potential for introducing defects required by Si-based optoelectronic devices. Recently, Bao *et al.*[14] has demonstrated W-line LEDs using a combination method of ion implantation, pulsed laser annealing and rapid thermal annealing at 275 °C. R-line and D1-band have also been reported after ion implantation of Si^+ into Si bulk but there is no systematic investigation on the formation of corresponding defects, as a function of the implantation dose and the annealing conditions. In the active layer of LEDs, the concentration and position of these defects have to be well controlled. In this work, we systematically varied the ion implantation dose and annealing temperature, and investigated their effect on the distribution of luminescence centers, which were probed by depth-dependent photoluminescence (PL) technique.

II. EXPERIMENTS

Double-side polished and B-doped silicon wafers (100) with resistivity ~10 Ω cm were implanted at room tempera-

[a)]Electronic mail: yuyang@ynu.edu.cn.
[b)]Electronic mail: cwang6@163.com.

ture with the implantation energy of 300 keV and the $^{28}Si^{+}$ ion doses of 10^{14}, 3×10^{14}, 10^{15}, and 3×10^{15} cm^{-2}. All implantation were carried out at 7° from normal to minimize channeling effects. The average projected range (R_p) is around 405 nm for the 300 keV Si^{+} ions, which was determined by the Monte Carlo simulation program (TRIM). Subsequently, the irradiated samples were cleaved into pieces and then were annealed in a conventional furnace tube with the flowing ultrahigh pure N_2 gas. Temperature range for the annealing experiments is from 300 to 950 °C. All the samples were loaded to the furnace at room temperature, and then ramped up to the preset temperature at the constant rate of 20 °C/min. After keeping the preset temperature for 30 min, the samples were cooled naturally to room temperature with the protection of the flowing N_2 gas. In order to obtain the depth profile of the defects responsible for the respective luminescence, the Si surface layer was removed step-by-step by using the reactive ion etching (RIE) technique. The PL from the samples was excited by a 458 nm argon laser, dispersed by a monochromator (JY Horiba, Triax 550) and detected by a cooled InGaAs detector. The standard lock-in technique was used to improve the signal to noise ratio. In the PL experiments, the samples were mounted on the cold tip of optical cryostat cooled by continuous flow helium. It allows the temperature for the optical measurements to be varied from 6 to 300 K. The absorption depth at 458 nm in crystalline silicon is estimated to be around 700 nm, defining the maximum penetration depth in all samples since the optical absorption will increase with defect density.

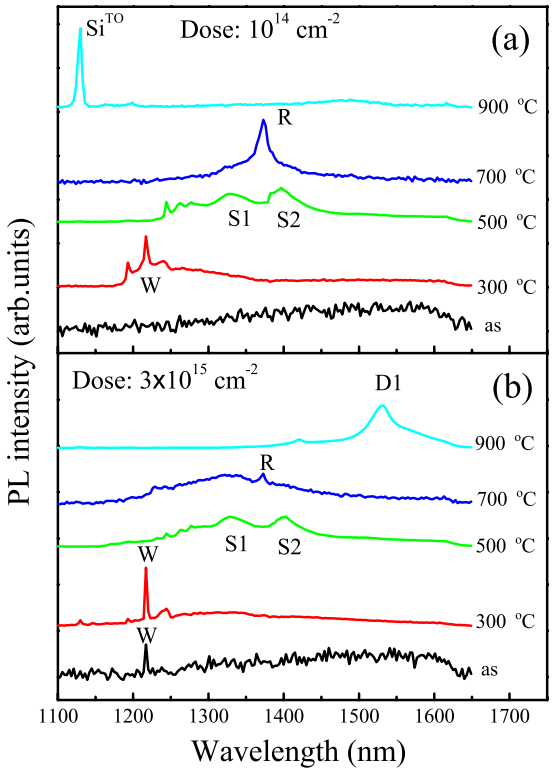

FIG. 1. (Color online) PL spectra of the samples annealed for 30 min at temperatures from 300 to 900 °C. Spectra at the bottom of (a) and (b) were taken from samples before annealing. The spectral signals were recorded at 7 K. The samples were implanted with Si^{+} doses of (a) 1×10^{14} cm^{-2} and (b) 3×10^{15} cm^{-2} at 300 keV in p-type silicon wafers. Vertical scales are arbitrary with respect to one another; spectra are shifted vertically for clarity.

III. RESULTS AND DISCUSSION

Figure 1 shows the PL spectra of the samples implanted at the lowest dose of 1×10^{14} cm^{-2} (a) and the highest dose of and 3×10^{15} cm^{-2} (b), and annealed at 300 °C, 500 °C, 700 °C, and 900 °C, respectively. The PL intensity is very weak or undetectable for those unannealed samples. After annealing at the temperature around 300 °C, the intensity of W-line (at ~1.22 μm) reaches its maximal, while this feature disappears if the annealing temperature is around 500 °C and above. The R-line (1.37 μm) defects begin to form when the annealing temperature reaches 700 °C. At 900 °C, the D1-band (~1.55 μm) luminescence dominates the PL spectrum of the sample with the highest dose in Fig. 1(b). Two broad peaks, S1 and S2 centered at ~1.32 μm and ~1.4 μm, respectively, start to appear in the PL spectra when the annealing temperature is above 350 °C. They have been tentatively attributed to the strained regions surrounding the interstitial clusters in the silicon matrix, which are precursors of the R-line centers.[13] In order to obtain a better understanding of the transition from the R-line to the D1-band, we performed annealing experiments at 700, 750, and 800 °C for all the samples, as shown in Fig. 2. It exhibits in Fig. 2(a) that the R-line of these samples annealed at 700 °C has the strongest intensity at the lowest dose of 10^{14} cm^{-2}. A well-defined D1 feature begins to appear at 800 °C and with a minimum implantation dose of 3×10^{14} cm^{-2}, as shown in Fig. 2(c). The PL spectra of the samples with an intermediate annealing temperature (750 °C) are shown in Fig. 2(b), where the intensity of R-line decrease with the increase in the dose and the D-line only presents in the sample with the dose of 3×10^{15} cm^{-2}.

In order to obtain the defect distribution for the W-line, R-line, and D1-band, the PL experiment was performed after every RIE removal of ~200 nm layer from the silicon wafer surface. Figure 3(a) shows the depth-dependent PL spectra of R-line, of which the sample was annealed at 700 °C for 30 min with the implantation dose of 10^{14} cm^{-2}. Presumably, the RIE process does not leave large-size surface textures, which may affect its optical absorption coefficient and corresponding PL intensity. It is also worth noting that there is negligible effect introduced by the RIE process to the luminescence signal of band edge and defects in the virgin silicon wafer, it had been demonstrated in our previous experiments (not shown). After the top 600 nm Si layer removed, the intensity of R peak is about 20 times stronger than that measured before RIE removal. Figure 3(b) shows the depth profiling results of the sample annealed at 850 °C with a dose of 3×10^{15} cm^{-2}, where only the D-line presents. Unlike R-line, the D1-band already shows a significant PL even without RIE removal, reaches its maximum after removing ~200 nm top Si layer, and becomes negligible after etching off 600 nm silicon. The depth-dependent results of PL experiments for R-line, D1-band, as well as W-line are summarized in Fig. 4.

It is noted that the dependence of the PL intensity and the luminescence defect concentration on the depth are re-

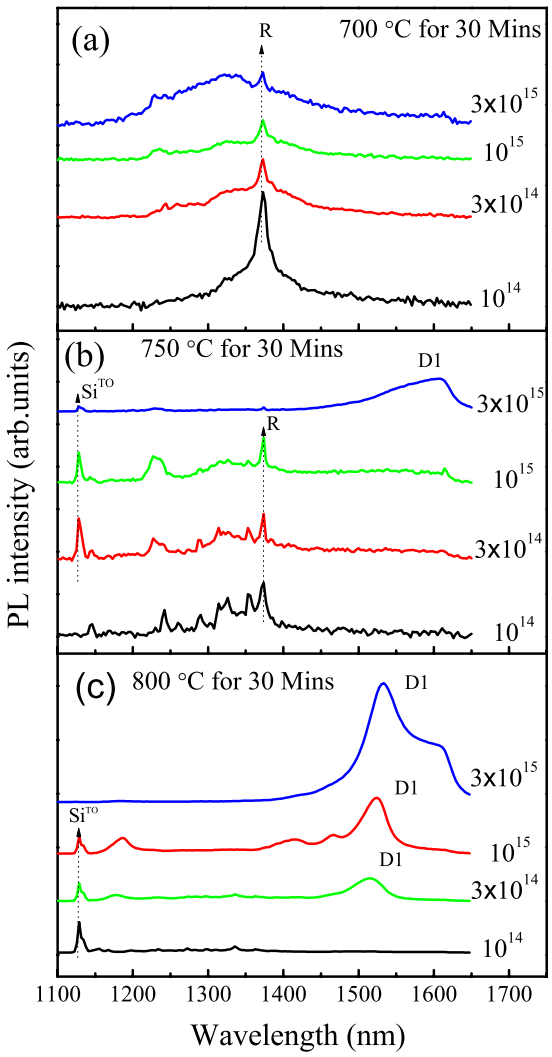

FIG. 2. (Color online) An overview of PL spectra at 7 K from the samples implanted with doses from 1×10^{14} to 3×10^{15} cm^{-2} and annealed for 30 min at (a) 700 °C, (b) 750 °C, and (c) 800 °C. All vertical scales are identical within each panel; the spectra are shifted vertically for clarity.

lated to each other but not identical. A precise determination of spatial distribution of luminescence defects requires a better knowledge of the spatial variation in the optical absorption constant, the carrier diffusion rate, and the electron-hole recombination rate in the ion damaged silicon. These properties strongly depend on the types of defects and their concentrations. For example, the weak PL intensity of W-line before RIE is mainly caused by the strong optical absorption of the excitation laser by the surface amorphous layer, which is known to form for an ion implantation dosage in excess of 10^{14} cm^{-2}, and does not recrystallize after annealing at temperatures below ~500 °C. Despite these complications, the defect distribution can still be roughly estimated. The initial increase in the PL intensity before reaching its maximum is due to the removal of a silicon layer which strongly absorbs incident excitation light but contains no or negligible luminescence defects or due to the removal of nonradiative recombination centers.[19] On the other hand, the decrease in PL intensity after the maximum can be ascribed to the removal of luminescence defects contained in that layer. Therefore, the peak concentration of luminescence centers were deter-

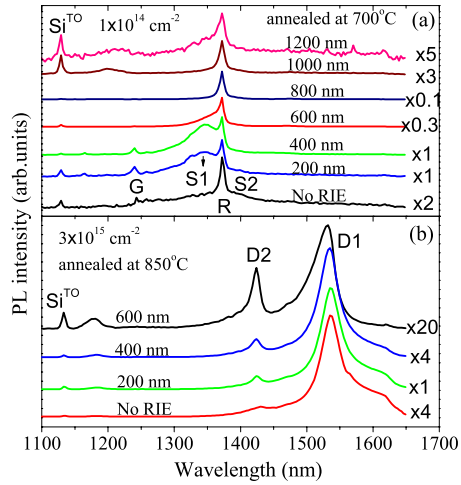

FIG. 3. (Color online) PL spectra after the removal of top layers at different thickness. All measurements were performed at 7 K, and all vertical scales are same within each panel. (a) Depth-dependent PL from the sample implanted with a dose of 1×10^{14} cm^{-2} and annealed at 700 °C for 30 min. (b) Depth-dependent PL from the sample implanted with a dose of 3×10^{15} cm^{-2} and annealed at 850 °C for 30 min.

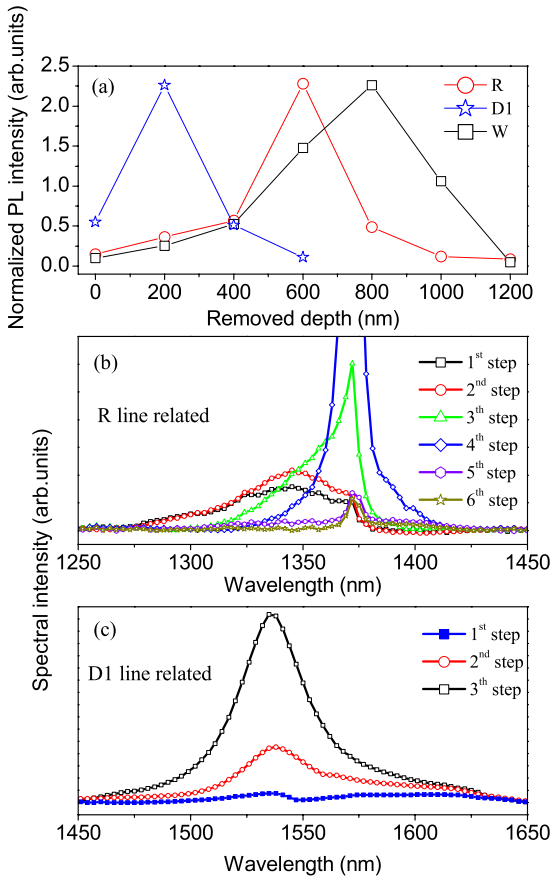

FIG. 4. (Color online) (a) Normalized PL intensities of W-line, R-line, and D1-line vs etch depth. The intensities of R-line and D1-line are taken from Figs. 3(a) and 3(b), respectively. W-line sample was implanted at a dose of 3×10^{15} cm^{-2} and annealed at 275 °C for 30 min. (b) and (c) refer to difference spectra obtained by subtracting the PL spectra for each RIE removed step related to the R-line (b) and D1-line (c) in Figs. 3(a) and 3(b), and corrected in such way that the spectra intensity at the fixed wavelength is proportional to the average concentration of R, S1, S2, and D1 defects emitting at that wavelength, respectively.

mined by the maximum decrease rate of PL intensity as a function of etch depth and it is always located beyond the peak position of PL intensity. For example, the W-line intensity reaches its maximum after removal of ~800 nm of silicon, and it decreases by 80% after further removal of ~400 nm of silicon. From this observation, it was concluded that the W-line defects are concentrated in a region of 800–1200 nm from the surface. In other word, the depth (~1000 nm) of the maximum concentration of W-line defects is deeper than that of its maximum PL intensity (~800 nm). Likewise, the defects responsible for the R-line are mainly distributed at ~700 nm from the surface. The D1-band defects were distributed in a range of 200–600 nm from the top surface. The large PL of D1-band before RIE is due to the fact that most of the ion implantation damage to the top silicon layer has been removed after annealing at 850 °C. The above discussion neglects the effect of nonradiative centers on the PL intensity of the luminescence centers. Strictly speaking, the maximum concentration of luminescence centers should be understood as the optimal concentration where the difference in concentration between luminescence centers and nonradiative centers reaches the maximum. In practice, this information is most essential for device design and fabrication.

Considering the different diffusion length of the carrier, one also could extract the exact distribution of the concerned defects as a function of depth by using the deconvolution method introduced by Brongersma, *et al.*[20] Figures 4(b) and 4(c) show the corrected difference spectra of Figs. 3(a) and 3(b), ordered according to the layer was etched off, respectively. For each etch step one can clearly see whether and how many the luminescence centers were removed with the corresponding Si layer. For instance, the steeply increase and decrease in the R-line related difference spectra occur during the third and fifth etch step in Fig. 4(b), respectively. This means that most of R centers are located in the surface depth range of 600–1000 nm. The monotonous increase in the difference spectra intensity from first to third etch step has been shown in Fig. 4(c). The largest increase in the spectral intensity at D1-line occurs during the third etch step, this implies that almost all the D1 centers are distributed in the depth range of 400–600 nm. These results derived from the deconvolution method agreed well with our estimation on the defect depth profile mentioned in the previous paragraph. In addition, the depth distribution of S1 and S2 centers also can be concluded based on the difference spectra in Fig. 4(b). Most of the S2 defects are accumulated at the ~800 nm under the surface, while almost all the S1 centers are distributed in a shallower and wider range of 0–600 nm.

Both R-line and W-line defects are Si-interstitial clusters, whose exact atomic configurations are still controversial. It has been proposed that small interstitial complexes, either tri-interstitials (I_3) or tetrainterstitial (I_4),[21,22] are responsible for the W-line. From the simulation, three different regions are created after ion implantation. The simulations based on FASTRIM program indicate that vacancies, created by ion due to the knock-out effect, mainly present in the region above R_p (~400 nm), while a large number of Si interstitials can be found in the region below R_p. Here, FASTRIM is a modified version of TRIM-90 that takes into account the multilayer target (interfaces) problems inherent with TRIM. The region near the R_p not only contains a high concentration of self-interstitials, but also suffers the maximum lattice damage. During thermal annealing, small clusters of interstitials migrate and agglomerate into larger clusters of interstitials. Therefore, it explains the experimental observation that both the R-line and W-line defects mainly locate below the projected ion range R_p. The maximum concentration of W-line defects locate at about twice of the R_p, which is believed to be a combined results of less lattice damage or less nonradiative centers, a high initial concentration of interstitials and their activation and migration process during the thermal annealing.

The R-line is believed to originate from the extended defects. The 300 keV Si ion implantation process was also simulated by using the FASTRIM software. The calculated results indicate that the location of the highest defect concentration conincides with the peak concentration position of the W and R defects estimated from the RIE depth profiling results, which suggests that the sources for W-line and R-line are interstitial-related defect clusters or the localized lattice strain. The source of D1-line is still debatable, i.e., whether it is from relaxed dislocations or associated point defects in between the dislocations. In our depth profiling study, the intensity of D1-line dropped before the dislocations were removed, which seems to support the latter.

Figure 5 shows the PL spectra of W-line, R-line, and D1-band at several representative temperatures, respectively. All the three signatures reveal the thermal quenching effect to some extent. The intensity of W-line drops dramatically when temperature rises above 40 K, while the R-line intensity remains almost the same at least at temperatures up to 80 K, as shown in Figs. 5(a) and 5(b), respectively. It is interesting to note in Fig. 5(c) that the thermal quenching seems to show less effect on the intensity of the D1-band, which is still clearly detectable at 220 K. Figure 6 shows the Arrhenius plot of the intensity (I) versus the measurement temperature (T) from 7 to 280 K. Among all the three optical features, D1-band exhibits the maximum intensity in the concerned temperature range. This is probably due to a less severe thermal quenching effect and the related impurity gettering process. According to these PL experimental results, a room-temperature D1-band LED can be expected based on the self-ion-implanted silicon.[18] The activation energy (E) values for D1-band, W-line, R-line are 186 meV, 50 meV, and 26 meV, respectively, which were obtained by fitting the plots to an Arrhenius form, i.e., $I(T) \sim \exp(E/k_B T)$ with k_B the Boltzmann constant.

IV. CONCLUSION

We systematically investigated the effects of ion implantation dosage and annealing temperature on the formation and distribution of three strongest luminescence centers. D1-band redshift and lines widen with the increase in implanted doses. High dose also catalyze PL peak transforms from R-line to D1-band. When the sample annealed at lower temperature (≤650 °C), the PL features exhibit larger different

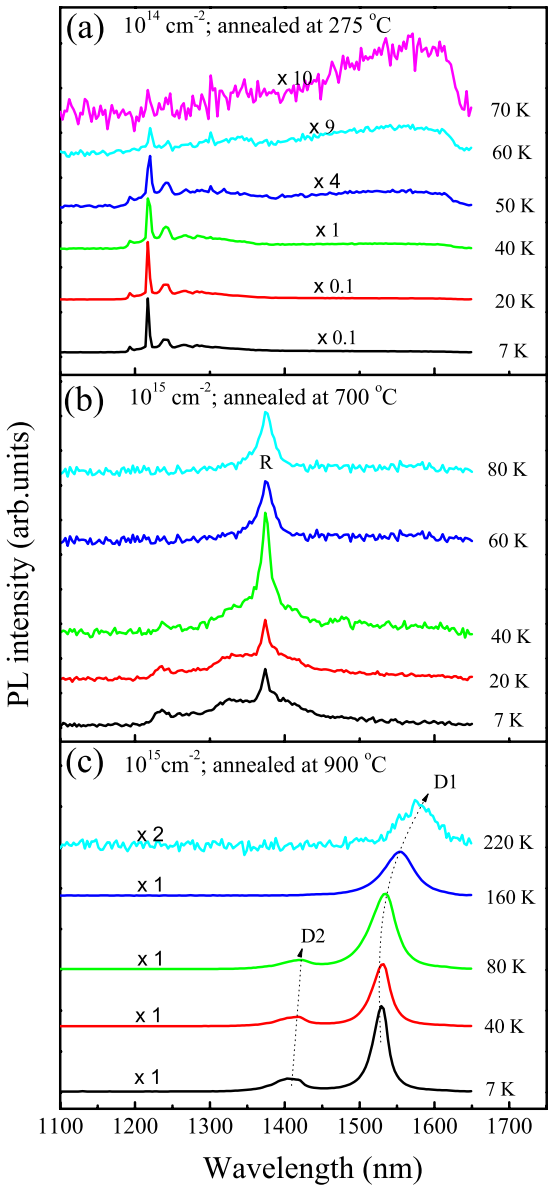

FIG. 5. (Color online) PL spectra involved the W-line, R-line, and D1-band measured at different temperatures. (a) W-line sample implanted to dose of 1×10^{14} cm^{-2} then annealed at 275 °C for 3 min. (b) R-line sample implanted to dose of 1×10^{15} cm^{-2} then annealed at 700 °C for 30 min. (c) D1-band sample implanted to dose of 1×10^{15} cm^{-2} then annealed at 900 °C for 30 min.

that are resolved sever peaks origin from point defects at low recorded temperatures and changed into broadband luminescence origin from cluster defects at high recorded temperatures. However, when the sample annealed at higher temperatures (>650 °C), the features of PL lines are similar at different recorded temperatures but D1-band undergoes a redshift and broadening with increasing recorded temperatures. By studying the evolution of PL spectra of these samples before and after etched off, the depth resolved information is obtained on the location of all the luminescence centers in the implanted samples. The locations of defects, in comparison with simulation, indicate that they originate from the interstitials and dislocations. Our study on the interstitial defects provides basic knowledge for fabrication of the defect-engineered silicon-based light emitting devices.

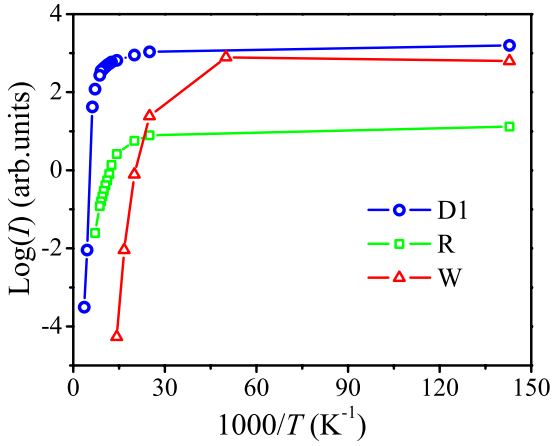

FIG. 6. (Color online) The Arrhenius plots of temperature-dependent PL intensities of the W-line, R-line, and D1-band, respectively.

ACKNOWLEDGMENTS

The PL measurements were performed at the laboratory of Professor Fedrico Capasso. We thank S. Charnvanichborikarn in the Australian National University for ion implantation of all samples. The authors would like to thanks Dr. H. T. Wang for assistance in the calculation of the intensity of PL peaks. One of the authors (Yu Yang) acknowledges the funding support of Natural Science Foundation of China under Grant No. 10964016 and the program of study abroad in Yunnan Province of China. It is a pleasure to thank Professor Jun Lin in the Smithsonian institution, Dr. Weiei Gao in Friend Laboratory, Dr. Lei Xu in Weitz group, and Dr. Xi Wang in Harvard University for their fruitful discussions.

[1]S. Ossicini, L. Pavesi, and F. Priolo, *Light Emitting Silicon for Microphotonics*, Springer Tracts in Modern Physics Vol. 194 (Springer-Verlag, Berlin, 2003).
[2]L. Pavesi, J. Phys.: Condens. Matter **15**, R1169 (2003).
[3]L. Pavesi, Mater. Today **8**, 18 (2005).
[4]Z. H. Lu, D. J. Lockwood, and J. M. Baribeau, Nature (London) **378**, 258 (1995).
[5]B. Zheng, J. Michel, F. Y. G. Ren, L. C. Kimerling, D. C. Jacobson, and J. M. Poate, Appl. Phys. Lett. **64**, 2842 (1994).
[6]M. C. Bost and J. E. Mahan, J. Appl. Phys. **58**, 2696 (1985).
[7]T. G. Brown and D. G. Hall, Appl. Phys. Lett. **49**, 245 (1986).
[8]G. Davies, Phys. Rep. **176**, 83 (1989).
[9]S. G. Cloutier, P. A. Kossyrev, and J. Xu, Nature Mater. **4**, 887 (2005).
[10]R. E. Harding, G. Davice, S. Hayama, P. G. Coleman, C. P. Burrows, and J. W. Leung, Appl. Phys. Lett. **89**, 181917 (2006).
[11]R. Sauer, J. Weber, J. Stolz, E. R. Webber, K.-H. Küsters, and H. Alexander, Appl. Phys. A **36**, 1 (1985).
[12]E. Ö. Sveinbjörnsson and J. Weber, Appl. Phys. Lett. **69**, 2686 (1996).
[13]S. Coffa, S. Libertino, and C. Spinella, Appl. Phys. Lett. **76**, 321 (2000).
[14]J. Bao, M. Tabbal, T. Kim, S. Charnvanichborikarn, J. S. Williams, M. J. Aziz, and F. Capasso, Opt. Express **15**, 6727 (2007).
[15]X. Yu, W. Seifert, O. F. Vyvenko, M. Kittler, T. Wilhelm, and M. Reiche, Appl. Phys. Lett. **93**, 041108 (2008).
[16]W. L. Ng, M. A. Lourenco, R. M. Gwilliam, S. Ledain, G. Shao, and K. P. Homewood, Nature (London) **410**, 192 (2001).
[17]T. Trupke, J. Zhao, A. Wang, R. Corkish, and M. A. Green, Appl. Phys. Lett. **82**, 2996 (2003).
[18]V. Kveder, M. Badylevich, E. Steinman, A. Izotov, M. Seibt, and W. Schröter, Appl. Phys. Lett. **84**, 2106 (2004).
[19]H. Y. Fan and A. K. Ramdas, J. Appl. Phys. **30**, 1127 (1959).
[20]M. L. Brongersma, A. Polman, K. S. Min, and H. A. Atwater, J. Appl. Phys. **86**, 759 (1999).
[21]G. M. Lopez and V. Fiorentini, Phys. Rev. B **69**, 155206 (2004).
[22]A. Carvalho, R. Jones, J. Coutinho, and P. R. Briddon, Phys. Rev. B **72**, 155208 (2005).